α-Cyclodextrin Functionalized CdS Nanocrystals for Fabrication of 2/3 D Assemblies

Nicoletta Depalo,[†] Roberto Comparelli,[‡] Marinella Striccoli,[‡] M. Lucia Curri,*,[‡] Paola Fini,[‡] Livia Giotta,[§] and Angela Agostiano[†,‡]

Dipartimento di Chimica, Università di Bari, via Orabona 4, I-70126 Bari, Italy, CNR IPCF Sez. Bari c/o Dip. di Chimica, Università di Bari, via Orabona 4, I-70126 Bari, Italy, and Dipartimento Scienza dei Materiali, Università di Lecce, via Monteroni, I-73100 Lecce, Italy

Received: May 5, 2006; In Final Form: July 6, 2006

Different types of cyclodextrins (CDs) have been tested as mediators for the water phase transfer of organic-capped CdS nanocrystals (NCs), and αCD has been demonstrated to be the most effective system. The formation of a complex based on αCDs and colloidal NCs has been considered to be responsible for the phase transfer process and extensively investigated by optical, structural, and calorimetric measurements, as a function of the experimental parameters (pH and NC and CD concentration). A mechanism for the complexation phenomena has been suggested. The fabrication of 2/3 D supramolecular architectures has been proposed according to two different strategies. First, a layer-by-layer procedure has been used to obtain multilayered structures where polyelectrolyte layers have been intercalated with negatively charged αCD−CdS NC complexes by exploiting electrostatic interaction between polyelectrolyte and cyclodextrin OH groups. Second, a monolayer of CdS NCs has been deposited onto a self-assembled monolayer of sulfated CDs, thus combining the use of an electrostatic-force-based approach and host−guest chemistry. The important role played by host−guest interactions has then been revealed.

Introduction

In the last years, growing attention has been aroused by the development of new methods for the preparation of nanometric organic and inorganic structures to use as functional building blocks for the fabrication of complex materials. Different degrees of hierarchical organization of such nano-objects can give the access to novel nanoarchitectures and nanodevices,[1−3] possessing unique properties which can be a function of the size, composition, and structural order. Indeed, nanosized particles can play a twofold role, exhibiting distinctive electronic,[4] optical,[5] and catalytic[6] properties, which originate from their quantum-scale dimensions[7] and are basically different from those presented by the corresponding bulk materials. In addition, such materials, aside from the peculiar properties of the individual non-interacting nanoparticles, are convenient structural elements and can effectively interact once assembled onto suitable substrates and/or organized in a defined assembly. From this perspective, these nanoelements become the objective of increasingly intensive investigation and growing expansion, with a fundamental role being played by their surface chemistry.

Over the past decade, considerable efforts have been devoted to the development of effective and reliable strategies for the fabrication and functionalization of colloidal nanoparticles, with tailored and predictable structural, optical, and surface properties. Modern materials science has actively investigated such functionalized colloidal nanocrystals, able to meet the increasing demands of structural and compositional complexity for their technological exploitation in areas linked to electronics, catalysis, and diagnostics. The design and engineering of such a class of materials are also interesting for the fundamental research in the field of colloidal materials and interface, since such nanoparticles can represent model systems to elucidate factors governing surface, interactions, and stabilization and to get a deep insight on their size dependent properties.

From this perspective, fabrication routes can be addressed to achieve ordered nanostructures by means of supramolecular chemistry and self-assembly of nanoscale process.

A plethora of approaches have been exploited in assembling nanoparticles, such as fluid-aligned,[8] surfactants-interacted,[9,10] DNA-directed,[10] electrostatic-interaction-oriented,[11,12] and recognition-mediated organization.[13] Self-assembled structures have also been successfully built up by exploiting the spontaneous control of noncovalent interactions between blocks, including van der Waals forces,[14] π−π interactions,[15] electrostatic forces,[16] and hydrogen bonding.[17]

In this work, oleic acid-capped CdS nanocrystals (NCs) have been synthesized and their surface properties have been tailored by using cyclodextrins (CDs) in order to modify their chemistry, functionality, reactivity, and surface charge, enhancing also their stability and dispersibility properties. The original host−guest characteristics of the CD functionalized CdS NCs have been in addition exploited for the fabrication of superstructures by means of different alternative strategies.

The CdS NCs have been synthesized with high control over size and size distribution by recently proposed colloidal chemistry routes,[18−20] and then, different types of cyclodextrin, namely, α, β, and γ, have been tested for the NC surface functionalization. CD is a class of molecule with torus-like macrorings built up from six, seven, and eight glucopyranose units, respectively, having a porous-shaped structure with a hydrophobic cavity and hydrophilic rims formed by hydroxyl groups; the former able to encapsulate small hydrophobic molecules and the latter effective in the solubilization in water.[21] The CD inclusion ability has been recently used to change the

* Corresponding author. E-mail: lucia.curri@ba.ipcf.cnr.it. Fax: +390805442128.
† Dipartimento di Chimica, Università di Bari.
‡ CNR IPCF Sez. Bari c/o Dip. di Chimica, Università di Bari.
§ Università di Lecce.

α-Cyclodextrin Functionalized CdS Nanocrystals

J. Phys. Chem. B, Vol. 110, No. 35, 2006 **17389**

solution properties of modified iron oxide nanoparticles by phase transfer between organic phase and aqueous solution[22,23] and to organize Au nanoparticle assembly.[24−26] Moreover, self-assembled monolayers (SAMs) of suitably modified CDs can be used as a host template to immobilize guest molecules.[27−31]

In this paper, the functionalization experiments by means of cyclodextrins (CDs) have demonstrated that αCDs are the best candidate to modify the surface properties of the oleic acid-capped CdS NCs, being a type of molecules that are able to solubilize them in aqueous solution without affecting their size and size distribution.

Finally, two different approaches to prepare hierarchical superstructures have been proposed. In the first procedure, αCD functionalized CdS NCs have been deposited onto substrates by electrostatic interaction using a polyelectrolyte-mediated layer-by-layer (LbL) method. The second approach has relied on the preparation of a monolayer of sulfated αCD (SαCD) onto a polyelectrolyte-modified quartz slide, which could be potentially exploited as a printboard for the deposition of αCD-modified NCs. The assemblies obtained with both of the investigated schemes have been characterized by IR multire-flectance spectroscopy and atomic force microscopy (AFM).

Experimental Section

Materials. All chemicals have been purchased with the highest purity available and used as received without further purification or distillation. Cadmium oxide (CdO, powder 99.5%), sulfur (S, powder 99.9999%), oleic acid (OLEA, technical grade 90%), octadecene (ODE, technical grade 90%), poly(allylamine hydrochloride) (PAH, MW = 70 000 g/mol), poly(sodium 4-styrene sulfonate) (PSS, MW = 70 000 g/mol), and α-cyclodextrin hydrate sulfated sodium salt (SαCD) have been purchased from Aldrich. Heptakis(2,6-di-*O*-methyl)-*β*-cyclodextrin (≥98%, HD*β*CD), heptakis(2,3,6-tri-*O*-methyl)-*β*-cyclodextrin (≥98%, HT*β*CD), hydroxypropyl-*β*-cyclodextrin (HP*β*CD; DS = 5.6), hydroxypropyl-*γ*-cyclodextrin (HP*γ*CD; DS = 4.8), *β*-cyclodextrin (*β*CD), and α-cyclodextrin (≥98%, αCD) were purchased from Fluka. All solvents used have been of analytical grade and purchased from Aldrich. All aqueous solutions have been prepared by using water obtained by a Milli-Q Gradient A-10 system (Millipore, 18.2 MΩ cm, organic carbon content ≤4 *μ*g/L) and filtered by 0.45 *μ*m nylon membrane filters (Whatman). Disposable dialyzer tubes (MWCO 3500) have been supplied by Aldrich.

CdS NC Synthesis. Organic-capped CdS NCs have been synthesized as reported elsewhere.[18−20] Briefly, the synthesis has been carried out under ambient conditions by heating at 300 °C a mixture of CdO, OLEA, and ODE with continuous stirring. The NC growth has been initiated by the injection of an ODE solution of elemental sulfur. The CdS NC yellow powder obtained after extraction and precipitation from the reaction mixture has been redispersed in hexane for the phase transfer experiments. The CdS NC concentration has been evaluated by absorbance spectra calculating the extinction coefficient as reported elsewhere.[32]

Phase Transfer. CD solutions in the concentration range from 8 to 20 mM have been prepared by using high purity water and filtered before the phase transfer process in order to remove possible CD aggregates. The CdS NCs in the hexane phase and CD aqueous solution have been mixed in a 1:1 ratio keeping the system at room temperature and under vigorous stirring for 20 h.[22,33,34] Finally, the water phase has been recovered by centrifugation and dialyzed versus Millipore water to remove the excess of CDs.

The phase transfer efficiency has been evaluated by estimation of three indirect parameters: depletion percentage, water soluble fraction, and insoluble fraction (eqs 1−3). The data have been obtained by the values of absorbance at the wavelength correspondent to the first allowed electronic transition of CdS NCs in the absorption spectra according to the following equations:

$$\text{depletion percentage (\%)} = \frac{A_{\text{hexane},t=0} - A_{\text{hexane},t=20\text{h}}}{A_{\text{hexane},t=0}} \times 100 \tag{1}$$

$$\text{water soluble fraction (\%)} = \frac{A_{\text{H}_2\text{O},t=20\text{h}}}{A_{\text{hexane},t=0}} \times 100 \tag{2}$$

$$\text{insoluble fraction (\%)} = \\ \text{depletion percentage} - \text{water soluble fraction} \tag{3}$$

All reported data are presented as mean values ± standard deviation obtained from five replicates.

Substrate and Monolayer Preparation. All of the solutions used have been freshly prepared. Quartz or silicon substrates have been negatively charged[35,36] by using an oxidative cleaning in "piranha" solution (OLEUM H_2SO_4 and 30% H_2O_2 in a 3:1 ratio; **CAUTION: Piranha solution reacts violently with most organic materials and should be handled with extreme care**) for 15 min and subsequently left in ultrapure water for 5 min. Finally, the substrates have been rinsed with acetone and dried with nitrogen.

The first polyelectrolyte layer has been deposited by dipping the quartz substrates in PAH solution (~1 × 10⁻⁵ M) for 10 min.[33,34] After rinsing with water, the slides have been immersed in the SαCD solution (~1 × 10⁻⁵ M in ultrapure water), for 10 min, exploiting the sulfated group negative charges.

After rinsing with a large amount of water, the substrates have been left in a solution containing a neutral αCD−CdS NC complex for 1 h. The slide has been rinsed with a large amount of water to remove physisorbed particles. This route has provided a quartz slide covered on both sides with a monolayer of NCs.

Multilayered Film Preparation. Multilayered structures consisting of a negatively charged αCD−CdS NC complex at pH 12 and polyelectrolyte layers have been prepared by a LbL approach.
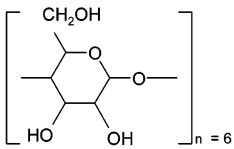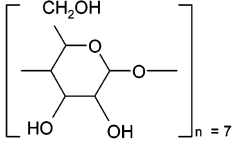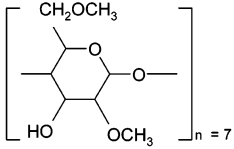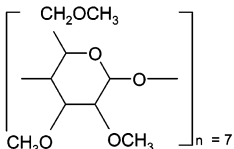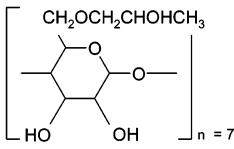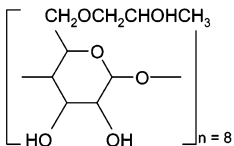
The procedure involves the alternate dipping of a silicon or quartz slide, previously cleaned with piranha solution, in the PAH and αCD−CdS NC (~10⁻⁶ M) solution, alternatively.[33,34] By this approach, both sides of the slide result in being covered with an assembly of the αCD−CdS NC stabilized nanocrystals onto the polyelectrolyte layer.

UV−Visible Spectroscopy. The phase transfer of CdS NCs from organic to aqueous phase and the self-assembly experiments have been both monitored by means of UV−vis absorption spectroscopy, by using a Varian Cary 5 spectrophotometer. The optical measurements on NC solution were performed at room temperature on the solution obtained directly from synthesis without any size sorting treatments.

IR Spectroscopy. Mid-infrared spectra have been acquired with a Perkin-Elmer Spectrum One Fourier transform infrared (FTIR) spectrometer equipped with a DTGS (deuterated trygli-cine sulfate) detector. The spectral resolution used for all experiments has been 4 cm⁻¹.

For attenuated total reflection (ATR) measurements, the internal reflection element (IRE) has been a three-bounce, 4 mm

TABLE 1: Experimental Values of Phase Transfer Obtained for the Investigated CDs under the Following Conditions: [CD] = 10 mM, [CdS NCs] = 10^{-6} M, NC Size = 3 nm

Name	Chemical Structure	Solubility (g/100ml)[41]	Depletion Percentage (%)	Water Soluble Fraction (%)	Insoluble Fraction (%)
αCD		14.5	100 ± 3	100 ± 3	0
βCD		2.0	52 ± 2	8.0 ± 0.2	44 ± 1
HDβCD		57	94 ± 3	1.0 ± 0.3	93 ± 3
HTβCD		31	39 ± 1	2.0 ± 0.1	37 ± 1
HPβCD		>60	63 ± 2	13.0 ± 0.4	50 ± 2
HPγCD		>50	50 ± 2	7.0 ± 0.2	43 ± 1

diameter diamond microprism. Cast films have been prepared directly onto the internal reflection element, by depositing the solution of interest (3−5 μL) on the upper face of the diamond crystal and allowing the solvent to evaporate completely.

A specular multireflection device designed specifically for thin film analyses (AmplifIR−SensIR technologies) has been employed for IR measurements on LbL films deposited onto Si slides. In this device, the IR beam is externally reflected between the sample surface and an adjustable gold-coated mirror. To analyze layers deposited on both the opposite faces of the support, a reflecting gold plate has been placed against the Si slide, which is transparent above 1300 cm^{-1}. According to the specular reflection principles and the geometry of the apparatus,[37] the IR beam passes through the slide, interacts with the layers deposited on both faces, and is then reflected by the Au plate toward the Au-coated mirror. The distance of the mirror with respect to the sample has been adjusted for achieving the maximum number of specular reflections of the beam before being conveyed to the detector.

Water Contact Angle Measurements. Water contact angle (WCA) measurements with water have been performed employing a Ramé−Hart contact angle goniometer (model A-100) in static mode and a standard goniometer. Each reported contact angle value is averaged for five measurements.

Calorimetric Measurements. Calorimetric measurements have been performed using an LKB 2277 (TAM) microcalorimeter equipped with a Thermometric 2250 titration unit. The experiments have been carried out by injecting 20 μL aliquots of a 35 mM αCD aqueous solution into the sample cell containing 1 mL of a αCD OLEA-capped CdS NCs complex aqueous solution ([αCD] = 8 mM and 2.8 nm NCs). Dilution experiments have been also performed. For this purpose, the measurements have been replicated by using 1 mL of an aqueous solution of 8 mM αCD to fill the sample cell.

Transmission Electron Microscopy. Transmission electron microscopy (TEM) images have been obtained using a JEOL 1100 microscope operating at 200 kV. The samples for the analysis have been prepared by dropping dilute solutions of CdS
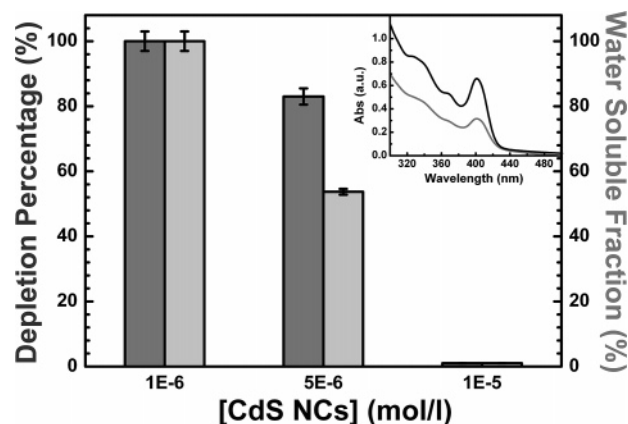
α-Cyclodextrin Functionalized CdS Nanocrystals

J. Phys. Chem. B, Vol. 110, No. 35, 2006 **17391**

Figure 1. Histogram of depletion percentage (dark gray) and water soluble fraction (light gray), CdS NC size 3.0 nm for different NC concentrations. Inset: Absorbance spectrum of water phase CdS NC starting from an initial CdS NC concentration in hexane of 5×10^{-6} M (black line) and 10^{-6} M (grey line).
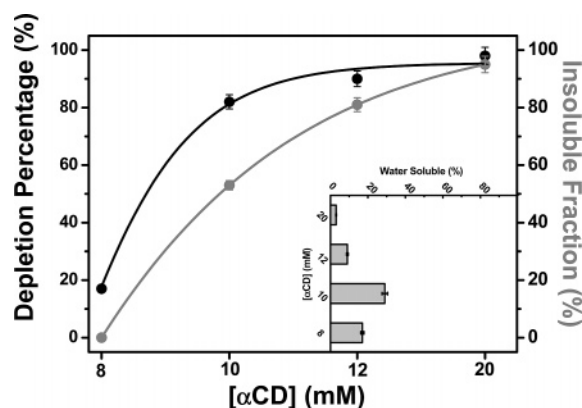

Figure 2. Diagram reporting the depletion percentage (black line) and the insoluble fraction (grey line) for the αCD−CdS NC complex vs [αCD]. Initial [CdS NC]$_{hexane}$ = 5×10^{-6} M, NC size = 3.0 nm. The solid lines are reported as guides for the eyes only. Inset: Water soluble fraction of the complex vs [αCD] obtained under the same conditions.

NCs or the αCD−CdS NC complex after dialysis onto 400-mesh carbon-coated copper grids and leaving the solvent to dry. The samples have demonstrated that they are stable under the electron beam, without degrading within the typical observation times.

Atomic Force Microscopy. Atomic force microscopy (AFM) experiments have been made with a PSIA XE-100 SPM system in AFM mode, and cantilevers with silicon nitride tips have been used. Topography images have been recorded in no contact mode at a 1 Hz scan rate with a resolution of 512×512 pixels.

Results and Discussion

CdS NCs have been prepared according to the literature by thermal decomposition of CdO and S.[18−20] Due to the synthetic procedure, the obtained NCs are coordinated by a layer of oleic acid, as demonstrated by IR measurements (see Figure 5).

The CDs demonstrated to be effective in modifying the CdS NC stability and dispersibility in different media and their surface reactivity by means of the formation of an inclusion complex. A detailed study of the phase transfer process, from organic phase to aqueous solution, has been performed as a function of several experimental parameters, namely, CD structure, NC and/or CD concentration, and pH of the CD solution. The formation of the NC complex has been monitored and extensively characterized by UV−vis absorption spectroscopy, IR-ATR spectra, and calorimetric measurements.
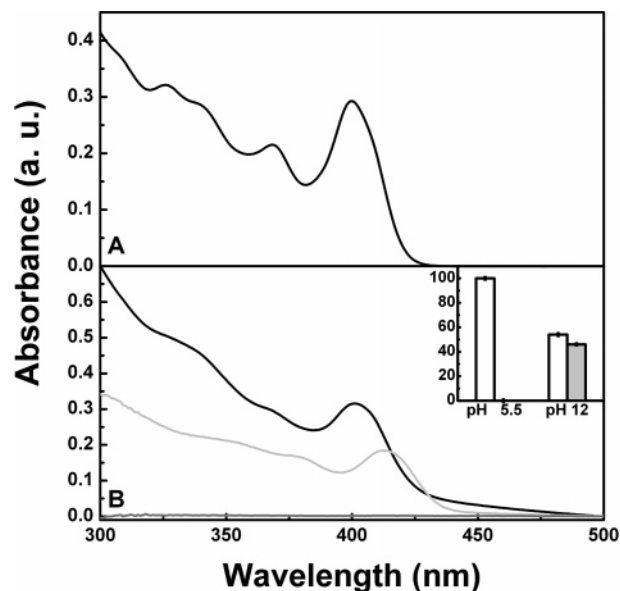

Figure 3. (A) Absorbance spectrum of CdS NCs in the hexane phase. (B) Absorbance spectra of the αCD−CdS NC complex in water at different pH values (black line, pH 5.5; light gray line, pH 12; dark gray line, pH 3). Experimental conditions: [αCD] = 10 mM, [CdS NCs]$_{hexane}$ = 10^{-6} M. Inset: Histogram of the NC water soluble fraction (white) and insoluble fraction (light gray) at different pH values.

In the second part of the paper, the assembly properties of the host−guest complexes have been exploited for the fabrication of hierarchical superstructures.

Effect of CD Structure. Different types of CDs (Table 1) have been tested in order to evaluate their suitability as host systems for the CdS NCs. Several CD derivatives, either naturally occurring, such as αCDs and βCDs, or obtained by modification of primary and secondary hydroxyl groups, have been tested, with the solubility of CD derivatives and the accessibility of their cavity being different from those found for their parent compounds, due to the different nature of the modifying group.[38]

A set of experiments has been performed by varying the CD concentration in the range from 8 to 20 mM, for all of the investigated CD types, and the summary of the results of the phase transfer experiments, obtained by the evaluation of the absorption spectra of the relevant samples, is reported in Table 1. In most of the cases, the formation of a translucent suspended material resulted. Such a suspended matter appears, however, to still be soluble in aqueous solution by the addition of water, according to what was previously reported for the αCD related experiments.[33,34] For this reason, the experimental data have then been evaluated by reporting the depletion percentage (representative of the extracted NCs from the organic phase), the water soluble fraction (representative of the amount of NCs observed in water after the phase transfer), and the insoluble fraction (representative of the suspended matter recovered at the interface). The accurate definitions of such factors are reported in the Experimental Section, together with their detailed explanation. The data reported in Table 1, relative to 3 nm CdS NCs ($\sim 10^{-6}$ M) and to 10 mM CD solution, clearly demonstrate that a successful phase transfer occurs only when αCD is used, with the water soluble fraction being equal to the depletion percentage. Similar trends have been observed for all the investigated CD concentration ranges explored (data not reported). βCD and the other modified CDs resulted in a less soluble complex, since only a negligible fraction of the complex has been effectively transferred in water.
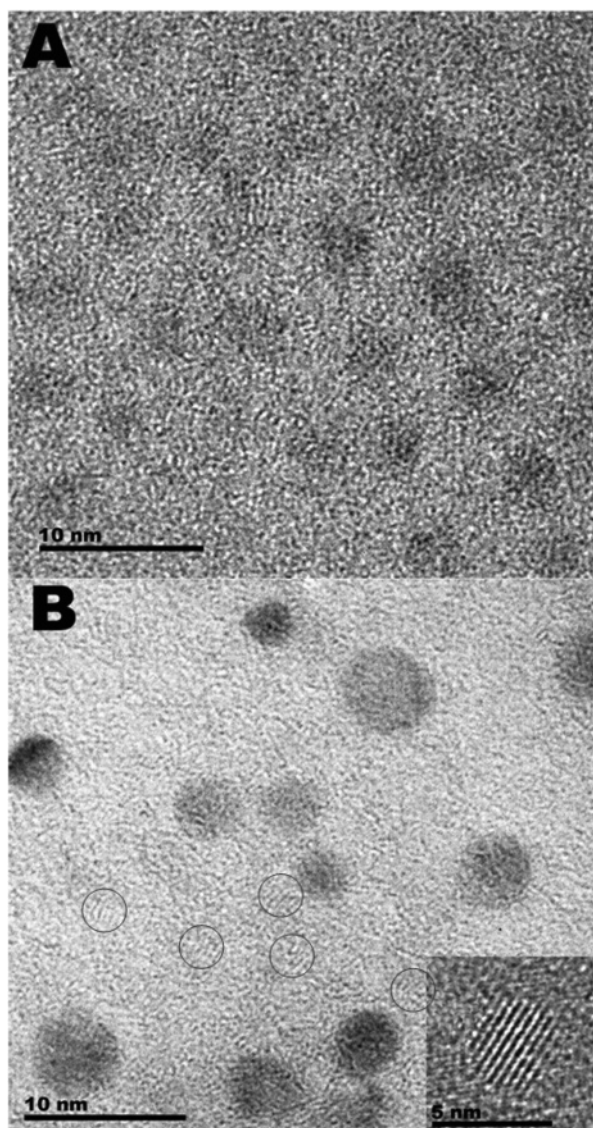
Figure 4. (A) TEM image of CdS NCs before the phase transfer, deposited from organic solution. (B) TEM image of αCD−CdS NCs deposited from water solution at pH 12. Inset: HRTEM picture of a αCD−CdS NC deposited from water solution at pH 12.

The results can be accounted for by the different nature of the CDs used and assuming that the interaction between the OLEA-capped CdS NCs and the CDs could involve essentially the alkyl tail of the organic acid. In general, acyclic guests are known to preferentially form an inclusion complex with αCDs rather than with βCDs, due to the different cavity size. This typical behavior could explain the higher effectiveness of αCDs with respect to βCDs in the phase transfer and also the difference in the achieved values of the water soluble fraction.[39]

HDβCD and HTβCD, where two and three OH groups, respectively, are replaced with CH_3O-, accomplish a value for the water soluble fraction of NCs that is lower than that found for the unsubstituted βCD. HPβCD, which presents a hydroxypropyl group in the C6 position, shows a slightly higher solubility in water than βCD, HTβCD, and HDβCD, thus suggesting that the hydroxypropyl group could be involved in the complexation of the OLEA alkyl chain on the surface of the nanocrystals by the CD. The low effectiveness of the γCD could be reasonably ascribed to its large cavity which could result in the formation of less stable complexes. In addition, the overall investigation suggested that the accessibility of the
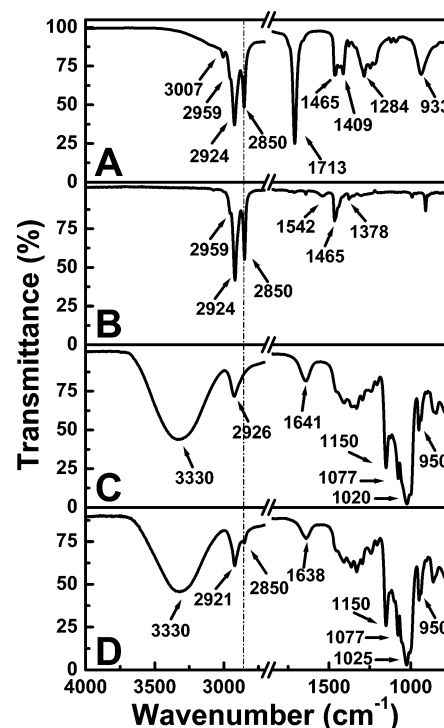

Figure 5. FTIR-ATR spectra of (A) pure OLEA, (B) OLEA-capped CdS NCs cast from hexane, (C) pure αCD cast from water, and (D) the αCD−CdS NC complex cast from water solution after a dialysis purification procedure.

modified CD cavity is generally reduced in reason of the steric hindrance of the substituent.

All of this evidence indicates αCD as the most suitable host to complex low molecular weight molecules, such as the carboxylic acid molecules, which represent the native capping layer at the NC surface.[22,38,40]

Effect of NC and CD Concentrations. The effect of the initial CdS NC concentration has been investigated in the range from 10^{-6} to 10^{-5} M at four different values of αCD content (8, 10, 12, and 20 mM). The CdS NC concentration in solution has been calculated from absorbance spectra by using a proper calibration procedure, as reported by Yu et al.[32]

In Figure 1, the results obtained in experiments performed by using 10 mM αCD solution show that a complete phase transfer is achieved only in the case of the lower CdS NC initial concentration (1×10^{-6} M). Under this condition, a higher number of CD molecules are available per each NC and this reason can be responsible for a more efficient complexation of alkyl chains.

In addition, the experimental data (inset of Figure 1) indicate that the highest concentration of NCs in the water phase can be attained starting from a 5×10^{-6} M NC solution, despite the lower depletion percentage and the lower water soluble fraction recorded under this condition, compared to the other starting concentration values.

For this reason, the dependency of the phase transfer efficiency on αCD concentration has been studied by keeping the NC concentration fixed at 5×10^{-6} M (Figure 2). Figure 2 shows that the percentage of the NC extracted from the organic phase, as well as the corresponding insoluble fraction, increases as the αCD concentration augments. In fact, by increasing the CD concentration, a white solid, soluble by water addition, can be recovered at the interface. The formation of this suspended matter has been found to occur starting from a limit value of the water solubility of the complex, with this value probably

TABLE 2: IR Signals Detected in the Investigated Samples and Their Assignments

| OLEA (cm^{-1})	OLEA−CdS NCs (cm^{-1})	αCD (cm^{-1})	αCD−CdS NCs (cm^{-1})	assignment
		3330	3330	OH stretching
3007				CH of −CH=CH− stretching
2959	2959			CH$_3$ antisymmetric stretching
2924	2924	2926	2921	CH$_2$ antisymmetric stretching
2850	2850		2850	CH$_2$ symmetric stretching
1713				C=O stretching of OLEA dimer
	1542			COO$^-$ antisymmetric stretching
1465	1465			CH$_2$ bending
1409				COH bending in plane
1378	1378			CH$_3$ bending
1284				C−O stretching
		1150	1150	C−O−C antisymmetric stretching
		1077	1077	C−C/C−O streching
		1020	1025	C−C/C−O stretching
		950	950	O−H bending out of plane
933				COH bending out of plane
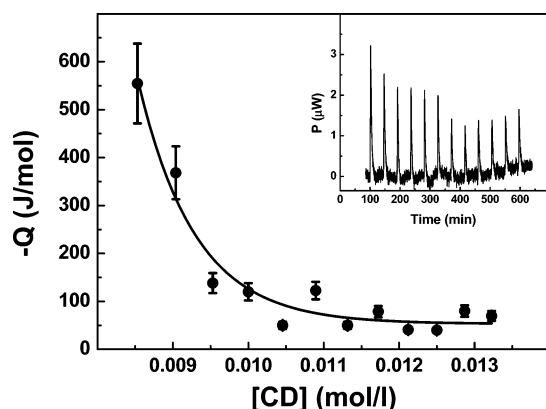
Figure 6. Diagram reporting the thermal effect associated with the interaction of αCD and the αCD−CdS NC complex at increasing αCD concentration. Inset: Experimental power−time plot associated with successive injections of an aqueous solution of 35 mM αCD to the aqueous solution of the αCD−CdS NC complex, obtained at [αCD] = 8 mM.

depending on the number of αCD molecules accessible per each single NC. In the inset, the values of the water soluble fraction have been reported as a function of CD concentration, pointing out that the experiments performed at [αCD] = 10 mM result in the highest value (∼30%).[33] The overall data indicate that an efficient phase transfer can only result in a proper ratio between NC and αCD concentrations. In fact, when the CD concentration is too low, no phase transfer has been registered, while an efficient depletion has been obtained for very high CD concentrations, although the resulting complex has been found to not be adequately stable in water. The most favorable [αCD]/[CdS NC] ratio for an effective phase transfer can be reasonably established corresponding to a value of ∼10 000.

Effect of pH. The effect of pH has been investigated by carrying out the phase transfer experiment by using the αCD solution at three different pH values (pH 3.0, 5.5, and 12.0, respectively). The αCD concentration has been varied in the range from 8 to 20 mM, with the pH of each αCD solution being adjusted by adding the proper amount of 0.1 M NaOH and HCl before the phase transfer.

In Figure 3, the absorption spectra of NCs in hexane before the phase transfer procedure and after the extraction in the aqueous phase are reported at different pH values. The optical measurements evidence that a complete phase transfer is obtained only in the case of neutral and alkaline solutions. At acid pH (pH 3), an extensive precipitation of NCs from the organic phase has been observed in the whole range of investigated αCD concentrations. In addition, the yellow solid

matter recovered at the bottom of the flask has resulted to be insoluble in water.

The yellowish appearance of the powder, differing from the white color observed in the previously described series of experiments (see section "effect of CD concentration"), could be indicative of the CdS NC aggregation.[7] This phenomena can be explained by an interaction between the double bond in the OLEA alkyl chain and NC surface which can be positively charged at acid pH. Such interaction can also reduce the capability of OLEA in preventing NC aggregation, according to the reported works on the interaction between OLEA and either ZrO$_2$ or TiO$_2$ in an aqueous environment.[42,43]

In addition, the pH value of the starting CD solution can alter the conformation of the OLEA, which could possibly lay aside instead of standing up at the NC surface, as expected in its extended conformation. In this way, the altered surface geometry of OLEA, and the consequently altered packing situation, could account for the unsuccessful phase transfer.

A complete extraction of the NCs from the organic phase as well as the evidence of a water soluble and insoluble fraction recounted in the range of 50% have been observed at alkaline pH. On the contrary, a 100% water soluble fraction has been recorded at neutral pH (inset of Figure 3B). A red-shift of the absorbance maximum occurring at basic pH (see Figure 3A and B for comparison) which is apparently indicative of a NC size enlargement is also revealed. Interestingly, any significant alteration in the NC size appears to occur at pH 12, as suggested by high resolution transmission electron microscopy (HRTEM) pictures of the αCD−CdS NC complex (see Figure 4), which also show the presence of a large amount of organic matter (the dark spots in Figure 4B) due to the free CD residuals. The detected red-shift in the absorption band could be explained by a different chemical environment surrounding NCs, in agreement with the recently reported data on water soluble CdTe NCs,[44] at alkaline pH. In our case, a modification of the local environment could be induced by the appearance of a negative charge due to the OH groups of αCD.[46] Moreover, a partial quenching of the band edge emission intensity at both alkaline and neutral pH has been observed.[33]

In addition, irrespectively of the pH value, the obtained samples have been found to be very stable in water for some time (at least 1 year), in contrast to the water soluble NCs functionalized with mercaptoalkanioc acids, which have been found to undergo aggregation after 1 week, being only stable in water at alkaline pH.[45]

FTIR Spectroscopical Investigation. Figure 5 reports the FTIR spectra recorded for OLEA, OLEA-capped CdS NCs, αCD, and the αCD−CdS NC complex, respectively. A sum-

CHART 1: Proposed Mechanism for the αCD−CdS NC Complex Formation
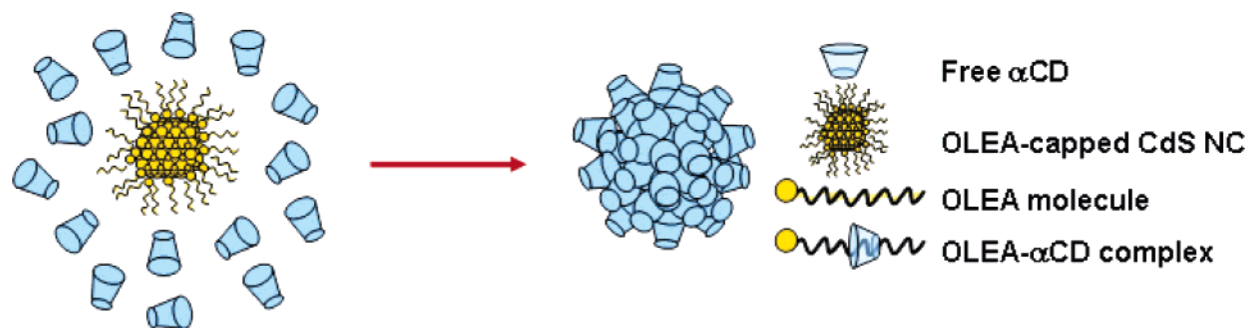
mary of the absorption band frequencies of the investigated samples, together with their assignments, is reported in Table 2.

Pure OLEA and OLEA-capped CdS NC samples both show three bands at 2959, 2924, and 2850 cm^{-1}, that are ascribable to the symmetric and asymmetric stretching of CH$_2$ and terminal CH$_3$ groups, respectively. In addition, the stretching of the olefinic CH bond is responsible for the band around 3007 cm^{-1}.

The presence of a carboxylic group is accountable for the strong band centered at 1713 cm^{-1} (stretch of protonated dimeric C=O), the weak band at 1409 cm^{-1} (in-plane bend of C−O−H), the weak band at 1284 cm^{-1} (stretch of C−O), and finally the signal at 933 cm^{-1} (out-of-plane bend of C−O−H) in the spectrum of pure OLEA.

The lack of these peaks in the spectra of the OLEA-capped CdS NCs is suggestive of an interaction between the carboxylic group and the NC surface, with the bidentate nature of such a bond being indicated by the presence of an asymmetric stretch of the COO$^-$ group at 1542 cm^{-1}.[42,43,47,48]

The spectra of pure αCD and the αCD−CdS NC complex (Figure 5C and D) are dominated by a broad strong absorption centered at 3330 cm^{-1}, typically ascribable to O−H stretching. The peak at 2926 cm^{-1} for the sample of the αCD−CdS NC complex, due to the asymmetric stretch of αCD CH$_2$ groups, is found to undergo a bathochromic shift of 5 cm^{-1} with respect to the signal of pure αCD.

In the αCD and αCD−CdS NC complex spectra (Figure 5C and D), three characteristic signals can also be observed: (i) the intense bands (1150, 1077, and 1020 cm^{-1}) assigned to the antisymmetric glycosidic C−O−C stretching vibrations and the coupled C−C/C−O stretch vibration,[22,24−26] (ii) the shallow band (1299−1460 cm^{-1}) assigned to the deformation vibrations

of C−H and O−H σ bonds of the CH$_2$ and OH groups, and (iii) the characteristic ring vibrations at 950 cm^{-1}. The signal at ∼1640 cm^{-1} arises from the scissoring mode of hydration water, which also contributes to the broad signal at ∼3300 cm^{-1} (symmetric and antisymmetric stretching modes of water OH). It has been indeed demonstrated that both of these signals are strongly affected by the hydration state of αCD (data not reported). Since cast films are prepared from aqueous solutions, it is reasonable that some water molecules are trapped and retained in the sample due to the hydrogen bonds established with αCD OH groups.

It is worth pointing out that the blue-shift at 1025 cm^{-1} of the C−C/C−O stretch vibration in the spectrum of the αCD−CdS NC complex[24−26] and the presence of the typical peak of the symmetric stretch of CH$_2$ in the alkyl chain of OLEA, missing in the case of pure αCD, are indicative of an inclusion-type interaction for the αCD−CdS NC complex.

Calorimetric Measurements. Calorimetric measurements have been performed in order to get additional insight into the interactions occurring between CD and organic-capped NCs, that possibly result in thermal effects. Such measurements can provide useful information on the stoichiometry of the complexation process.

The experiments have been carried out by filling the calorimetric cell with the aqueous solution of the OLEA-capped CdS NCs obtained from the phase transfer process with αCD. The αCD concentration (8 mM) used has been selected in order to achieve a significant concentration of NCs in the aqueous phase. The thermal effects, produced by performing a titration with a series of sequential injections of a 35 mM αCD solution into the calorimetric cell, have then been measured. Such a 35 mM αCD concentration has been suitably chosen in order to achieve, in the cell, a final plateau value of concentration corresponding to the quantitative transfer of CdS NCs in water.

The inset of Figure 6 shows the power/time plot associated with the above-described titration. Two control tests have also been performed in order to estimate the dilution contributions for the same experiment (data not reported).

The peak integration displayed in the inset of Figure 6 can provide an estimation of the heat associated with four different phenomena: The first two effects are due to the addition of the aliquots of 35 mM αCD solution and to the contribution ascribable to the concentration change in the initial 8 mM αCD solution. A further effect results from the dilution of the αCD OLEA-capped CdS NC complexes, and finally, another contribution is ascribable to the interaction occurring between the αCD and the OLEA-capped CdS NCs.

This last effect can be evaluated by leveling off the heat recorded in the blank experiment from the thermal effect evaluated in the titration experiment. Figure 6 shows the heat
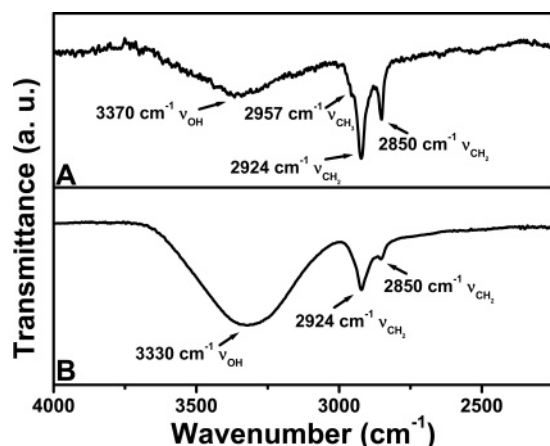

Figure 7. (A) IR spectrum of the multilayer assembly acquired by a multireflection system (see Experimental Section). (B) IR-ATR spectrum of the αCD−CdS NC complex cast from alkaline solution.
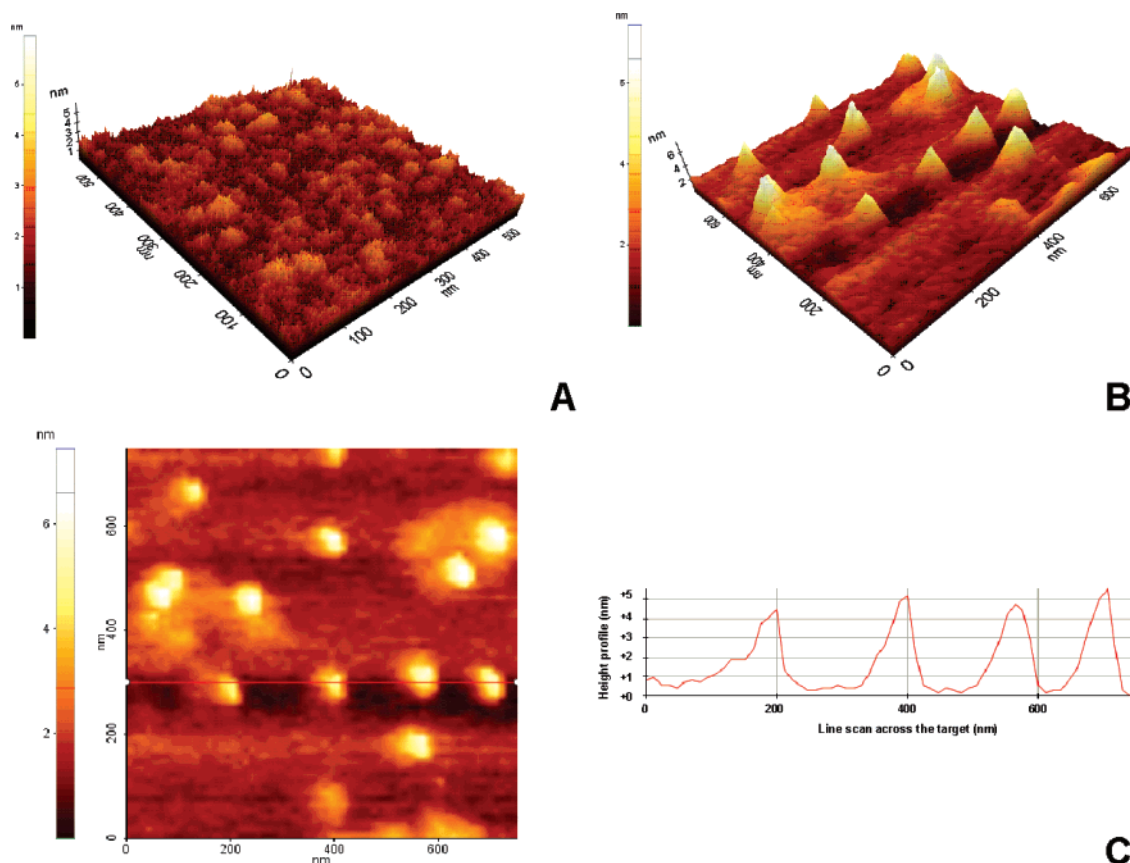
α-Cyclodextrin Functionalized CdS Nanocrystals

J. Phys. Chem. B, Vol. 110, No. 35, 2006 **17395**

Figure 8. AFM images of (A) 3D topography of bare silicon, (B) 3D topography of the same sample after the reported LbL assembly of αCD−CdS NCs (13 layers), and (C) line topography and height profile αCD−CdS NC LbL assembly.

due to the αCD−CdS NC interaction, as detected in the calorimetric cell at increasing αCD concentration.

In particular, the data reveal the occurrence of an interaction exothermic in nature, in agreement with the results reported for the binding of αCD to aliphatic alcohols.[49] In addition, the decrease of the amount of heat, recorded at increasing [αCD] in the cell, indicates a growing degree of occupancy of the NC binding sites, up to a saturation value, corresponding to the highest αCD−CdS NCs ratio in the complex.

The calorimetric experiments indicate that the phase transfer of OLEA-capped CdS NCs, carried out with a 8 mM αCD solution, results in the formation of a complex (Chart 1) which is still able to further interact with αCD molecules, accordingly with the already suggested dependence of the phase transfer efficiency on the αCD concentration.

Assembly Experiments. The αCD−CdS NC complex has been exploited for the fabrication of hierarchical superstructures by following two different approaches.

The first strategy is based on the preparation of multilayer assemblies consisting of the negatively charged αCD−CdS NC complex and the positively charged polyelectrolyte, poly-(allylamine hydrochloride) (PAH) layer, alternatively deposited in a LbL fashion. The electrostatic interaction between the negatively charged OH groups of αCDs, deposited from an alkaline solution, and the positively charged amine groups of PAH can act as a driving force for the deposition process. The occurrence of such specific interactions has been confirmed by a control test performed by replacing PAH with a negatively charged polyelectrolyte, poly(sodium 4-styrene sulfonate) (PSS) and ultimately resulting in the inhibition of the deposition process.

The deposition procedure has been monitored by means of UV−vis absorption spectroscopy and IR spectroscopy; for this
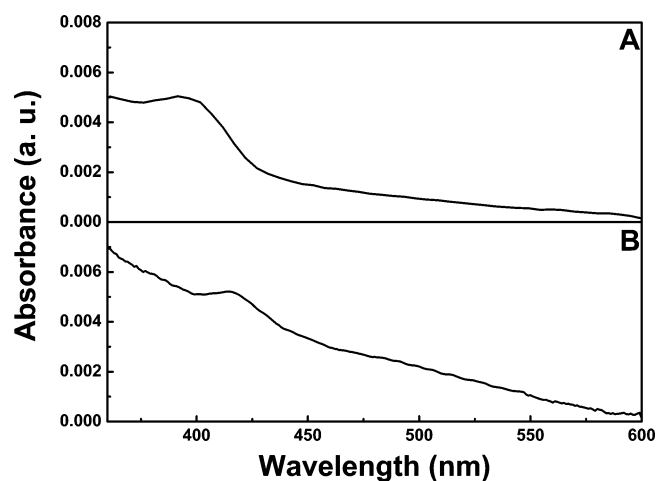

Figure 9. (A) Absorbance spectra of the αCD−CdS NC multilayer (20 layers) prepared by the LbL approach. (B) Absorbance spectra of the αCD−CdS NC monolayer prepared by using multivalent interactions.

TABLE 3: Contact Angle Measurements with Water

	right angle (deg)	left angle (deg)
clean quartz	60 ± 1	60 ± 1
quartz + PAH	87 ± 1	87 ± 1
quartz + PAH + SαCD	45 ± 1	45 ± 1

purpose, the multilayers were deposited onto both quartz and silicon substrates.

Absorbance spectra (data not reported) of the multilayered films demonstrated a linear dependence between the absorbance maximum intensity and number of bilayers.[33,34]

CHART 2: Proposed Binding Mechanism of a Multivalent Guest (OLEA-Capped CdS NCs) to Hosts (SαCD) Immobilized onto a PAH-Modified Slide
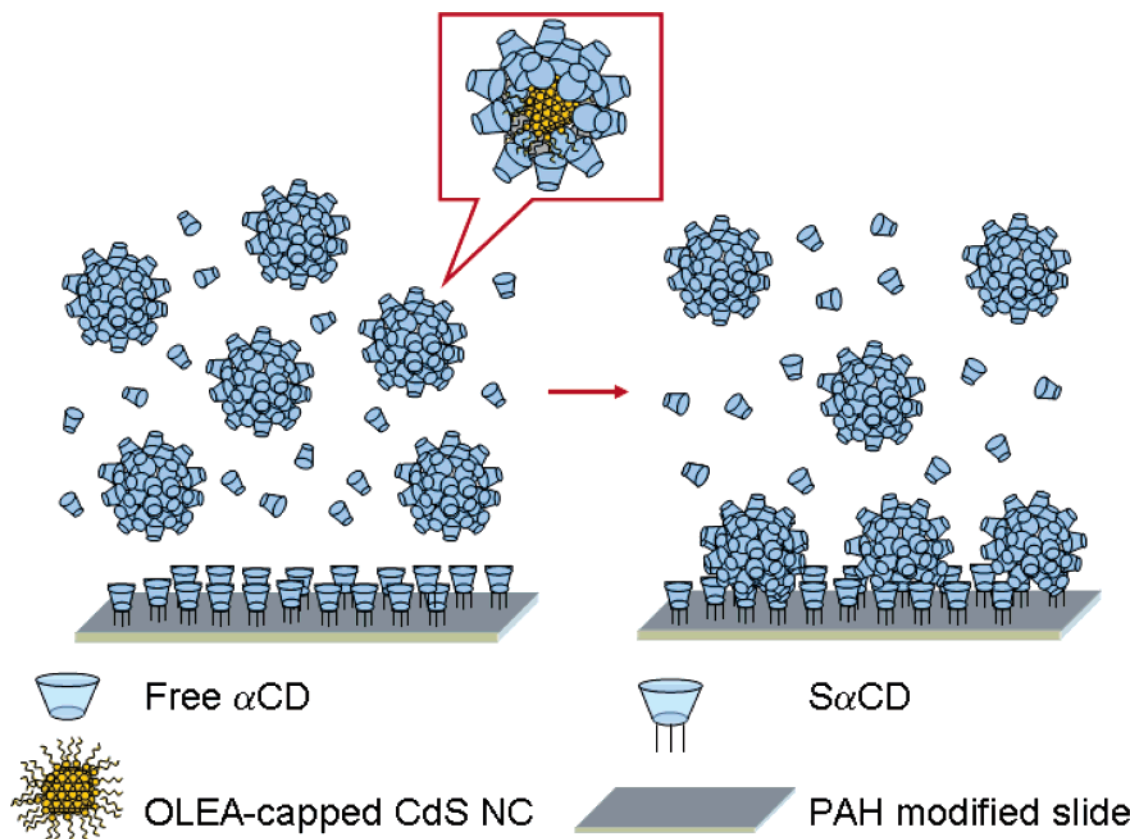
IR multireflectance spectroscopy measurements (Figure 7A) have been profitably used to prove the immobilization of the complex on the silicon substrate, as confirmed by the presence of the characteristic OH stretching mode (broad band at 3370 cm^{-1}) and by the signals due to the aliphatic carbon moiety (2850−2960 cm^{-1}).

The decrease in intensity of the αCD OH stretching signal with respect to the aliphatic CH band can be to some extent related to the partial deprotonation of the OH groups in the αCD at pH 12. Moreover, the significant decrease of this signal together with the shift at higher wavenumbers might be reasonably due to the extremely low amount of hydration water molecules in the LbL assembled film in comparison with the cast film (Figure 7). As already mentioned, it is likely that the disordered multilayered structure of cast films is associated with a higher content of trapped water molecules, so that the overlapping of αCD and water OH absorptions and the abundance of hydrogen bonds results in a more intense and broad band with a maximum centered at lower wavenumbers.

Notably, the multilayer assembly has been found to be very stable in time, since the absorbance spectrum and IR features remain unchanged after 3 months. In particular, the multilayer assembly appears stable against oxidative phenomena, with the absorbance maximum position being unaffected by the storage period in air.

Freshly prepared assemblies onto silicon have also been characterized by atomic force microscopy. The topography images reported in Figure 8A show the 3D morphological characteristic of a typical bare silicon substrate, after the treatment with piranha solution. The deposition of 13 layers of αCD−CdS NC complexes by the LBL procedure is reported to induce strong modifications in the surface appearance of the

sample, which are possibly ascribable to the immobilization of the functionalized NCs (Figure 8B).

The height profile registered on the substrate after LBL assembly shows the presence of dispersed objects, which results in an ∼5 nm size value that is in a good agreement with the value found by TEM analysis and with the expected dimension of the αCD−CdS NC complex (Figure 4B and ref 21). Lateral size values have not been taken into account, since such values are always overestimated due to known tip convolution effects. In fact, the true lateral resolution is limited by the radius of curvature of the tip, which for conventional AFM tips has values exceeding 15 nm, which is far larger than the expected nano-object size.[50] Interestingly, the NC-based complexes appear homogeneously dispersed and isolated on the substrate, without evident clustering or aggregation. Such behavior is consistent with the preservation of the NC characteristic optical properties, as confirmed by UV−vis spectra (Figure 9A).

The second assembly strategy is aimed to mix and match the electrostatic interaction strategy with multivalent host−guest interfacing in order to attain a hierarchal superstructure based on sulfated αCDs (SαCDs), which are preliminarily deposited onto PAH-modified suitable substrates and the subsequent formation of the αCD−CdS NC complexes (deposited from a solution at pH 5.5). SαCDs are known to possess the same cavity volume of native αCDs and present a negative charge due to the SO$_3^-$ substituent, which make them suitable for assembly by electrostatic interaction.[51] A monolayer of SαCD has been prepared by interaction with positively charged PAH amine groups, according to a previously reported procedure.[51] The successful accomplishment of this first step has been checked by contact angle measurements, as reported in Table 3, since a strong dependence of the surface wettability from
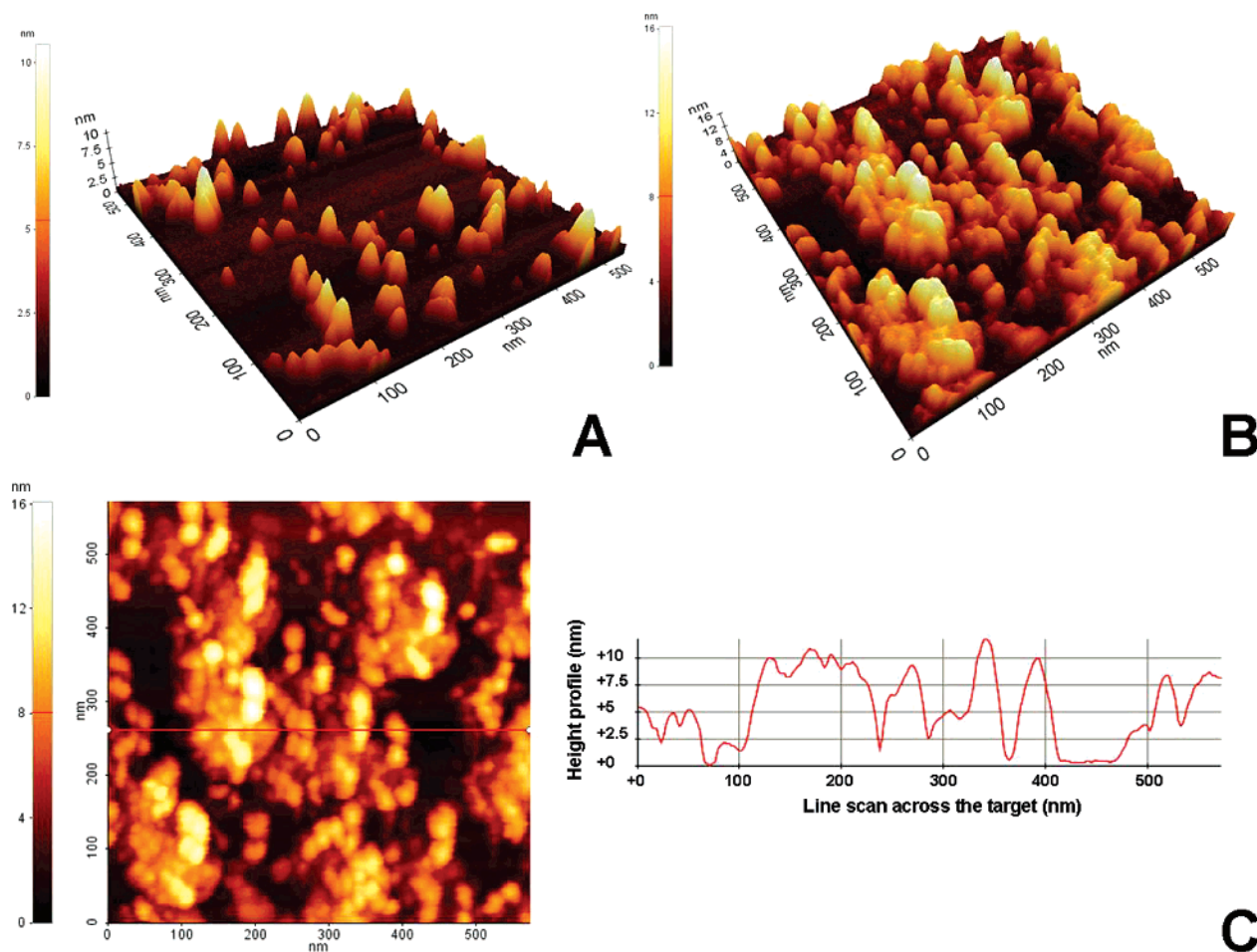
α-Cyclodextrin Functionalized CdS Nanocrystals

J. Phys. Chem. B, Vol. 110, No. 35, 2006 **17397**

Figure 10. AFM image of (A) the SαCD monolayer, (B) SαCD−CdS NC assembly 3D topography, and (C) SαCD−CdS NC assembly line topography and height profile.

the chemical groups present on the surface can be found. In particular, the treatment with piranha solution (see Experimental Section) followed by the PAH layer deposition results in a highly wettable quartz surface, which is strongly modified by the deposition of the SαCD immobilization, being then rendered slightly hydrophobic.

The as-prepared SαCD monolayer can act as a template for the immobilization of CdS NCs starting from the αCD−CdS complex. The success of this approach is confirmed by the UV−vis absorbance spectra (Figure 9B), that display the absorption band of the CdS NC exciton, even though a red-shift with respect to the same spectral feature in the sample prepared by the LbL approach can be noticed.

The SαCD immobilization process can be considered on the basis of multivalent host−guest interaction at interfaces. Monovalent ligands such as SαCD, immobilized onto the surface, can actually act as multivalent systems in complexing multivalent hosts.[27−30,52−55]

Free αCDs in solution could act as monovalent hosts and SαCDs monolayer as multivalent host system immobilized at the interface. The CdS NCs can thus be regarded as a multivalent guest, being the numerous OLEA alkyl chains at the NC surface considered each a guest site. The presence of an exchange equilibrium for the alkyl chains of the organic capping layer at the NC surface interacting either with the free αCDs or with the immobilized SαCDs allows the NC to participate in multiple interactions, which facilitate their immobilization onto the substrate. Although the strength of the interaction between each

NC monovalent guest site and SαCD SAMs is comparable to the strength of the interaction between the αCD in solution and the surfactant chain at the NC surface,[56] such a type of multivalent guest (such as organic-capped NCs) can interact much strongly with SαCD SAMs (Chart 2). This stronger interaction can be explained by the higher local concentration of hosts at the surface, that render such immobilized receptors a sort of multivalent system,[52,53] thus successfully competing with the monovalent hosts in solution, as accounted for also by the pertinent thermodynamic models.[52]

Recent papers report on the immobilization of cyclodextrin functionalized NCs prepared in aqueous media by exploiting multivalence interactions mediated by dendrimers which act as "glue molecules", able to bind both the NCs and the modified substrate.[57] In our scheme, a similar "glue" function is performed by the numerous OLEA molecules present on the NC surface owing to the synthetic procedure. In addition, the presented assembly procedure allows a host−guest chemistry driven immobilization of CdS NCs prepared with a well-established synthetic route, able to achieve a high control over NC size and size distribution.

AFM investigations have been carried out on the polyelectrolyte-modified silicon slide used as a substrate for SαCD deposition and on the same substrate after immobilization of the αCD−CdS complex (Figure 10). The image of the SαCD layer (Figure 10A) indicated a random distribution of objects in slightly differently populated regions. A similar distribution of objects has been reflected by the morphological features

recorded after the exposure to the αCD−CdS NC solution (Figure 10B and C). AFM images point out the formation of an assembly of the NC-based complex much denser than that observed in the case of the LbL deposition.

Such a crowded configuration and close packing of the NC can also be inferred by the height profile of the objects on the substrate, which give values (about 10 nm) not accountable by the presence of an isolated αCD−CdS NC complex. The occurrence of a specific absorption (i.e., physisorption) phenomena cannot be excluded, and could also be responsible for this evidence.

With such a close packed arrangement, NCs stay much closer to each other in this case, being thus in accordance with the red-shift recorded in the absorbance spectrum (Figure 9B) and possibly due to an energy transfer between NCs.[58]

Conclusion

The synthesized OLEA-capped CdS NCs have been successfully functionalized with CD, by efficiently exploiting their characteristic host−guest chemistry for the modification of the "as-prepared" colloidal NC surface and, accordingly, its properties. αCD has been found to be the most suitable host system, among all the inspected CDs, to complex the OLEA alkyl chain at the NC surface. The efficiency of a CD-mediated water phase transfer has been found to be dependent on the [αCD]/[CdS NC] ratio and on the pH value of the starting CD solution. The extensive spectroscopic (UV−vis and IR spectroscopies), structural (TEM), and calorimetric characterization of the complex has provided many useful insights on the types and strength of the interaction in the αCD−CdS NC complex formed.

The two different investigated deposition approaches have both achieved the preparation of the assembled structures based on the αCD−CdS NC complex. Namely, both the LbL procedure for fabricating a multilayer NC assembly onto solid substrates (quartz or silicon) by using PAH as the polyelectrolyte and the alternative deposition method, exploiting the strong interaction between monovalent SαCD-based hosts immobilized onto substrate and the αCD−CdS NC complex multivalent guest, have provided successful assembly results. The overall characterization results, obtained by UV−vis, IR multireflection, and AFM measurements, have contributed to the understanding of the features for the two types of assemblies, and of their peculiar properties. The long term stability of the prepared structures makes them an interesting candidate to develop systems and devices for nanoelectronic and nanobioelectronic applications.[59]

References and Notes

(1) Gopel, W.; Ziegler, C.; Breer, H.; Schild, D.; Apfelbach, R.; Joerges, J. Malaka R. *Biosens. Bioelectron.* **1998**, *13*, 479.

(2) de Silva, A. P.; Gunaratne, N. H. Q.; McCoy, C. P. *Nature* **1993**, *364*, 42.

(3) Lehn, J. M. *Angew. Chem.* **1990**, *29*, 1304.

(4) Khairutdinov, R. F. *Colloid J.* **1997**, *59*, 535.

(5) Mulvaney, P. *Langmuir* **1996**, *12*, 788.

(6) Lewis, L. N. *Chem. Rev.* **1993**, *93*, 2693.

(7) Alivisatos, A. P. *Science* **1996**, *271,* 933.

(8) Duan, X.; Niu, C.; Sahi, V.; Chen, J.; Parce, J. W.; Empedocles, S.; Goldman, J. L. *Nature* **2003**, *425*, 274.

(9) Hou, Y.; Gao, S.; Otha, T.; Kndoh, H. *Eur. J. Inorg. Chem.* **2004**, 1169.

(10) Aizenberg, J.; Black, A. J.; Whitesides, G. M. *J. Am. Chem. Soc.* **1999**, *121*, 4500.

(11) Mirkin, C. A.; Letsinger, R. L.; Mucic, R. C.; Storhoff, J. J. *Nature* **1996**, *382*, 607.

(12) Decher G., *Science* **1997**, *277*, 1232.

(13) Kolny, J.; Kornowski, A.; Weller, H. *Nano Lett.* **2002**, *2*, 361.

(14) Andres, R. P.; Bielefeld, J. D.; Henderson, J. I.; Janes, D. B.; Kolagunta, V. R.; Kubiak, C. P.; Mahoney, W. J.; Osifchin; R. G. *Science* **1996**, *273*, 1690.

(15) Jin, J.; Iyoda, T.; Cao, C.; Song, Y.; Jiang, L.; Li, T. J.; Zhu, D. B. *Angew. Chem., Int. Ed.* **2001**, *40*, 2135.

(16) Caruso, F.; Caruso, R. A. Mohwald, H. *Science* **1998**, *282*, 1111.

(17) Fyfe, M. C. T.; Stoddart, J. F. *Acc. Chem. Res.* **1997**, *30*, 393.

(18) Yu, W. W.; Peng, X. *Angew. Chem.* **2002**, *114*, 2474.

(19) Comparelli, R.; Zezza, F.; Striccoli, M.; Curri, M. L.; Tommasi, R.; Agostiano, A. *Mater. Sci. Eng., C* **2003**, *23*, 1083.

(20) Zezza, F.; Comparelli, R.; Striccoli, M.; Curri, M. L.; Tommasi, R.; Agostiano, A.; Della Monica, M. *Synth. Met.* **2003**, *139*, 597.

(21) Szejtli, J. *Chem. Rev.* **1998**, *98*, 1743.

(22) Wang, Y.; Wong, J. F.; Teng, X.; Lin, X. Z.; Yang, H. *Nano Lett.* **2003**, *3*, 1555.

(23) Lala, N.; Lalbegi, S. P.; Adyanthaya, S. D.; Sastry, M. *Langmuir* **2001**, *17*, 3766

(24) Hou, Y.; Kondoh, H.; Shimojo, M.; Sako, E. O.; Ozaki, N.; Kogure, T.; Ohta, T. *J. Phys. Chem. B* **2005**, *109*, 4845.

(25) Feng, J.; Ding, S. Y.; Tucker, M. P.; Himmel, M. E.; Kim, Y. H.; Zhang, S. B.; Keyes, B. M.; Rumbles, G. *Appl. Phys. Lett.* **2005**, *86*, 033108.

(26) Feng, J.; Miedaner, A.; Ahrenkiel, P.; Himmel, M. E.; Curtis, C.; Ginley, D. *J. Am. Chem. Soc.* **2005**, *127*, 14968−14969

(27) Crespo-Biel, O. Peter, M.; Bruinink, C. M.; Ravoo, B. J.; Reinhoudt, D. N.; Huskens, J. *Chem.−Eur. J.* **2005**, *11*, 2462.

(28) Onclin, S.; Mulder, A.; Huskens, J.; Ravoo, B. J.; Reinhoudt, D. N. *Langmuir* **2004**, *20*, 5460.

(29) Huskens, J.; Deij, M. A.; Reinhoudt, D. N. *Angew. Chem., Int. Ed.* **2002**, *41*, 4467.

(30) Beulen, M. W. J.; Bügler, J.; de Jong, M.; Lammerink, B.; Huskens, J.; Schönherr, H.; Vancso, G. J.; Boukamp, B.; Wieder, H.; Offenhäuser, A.; Knoll, W.; vanVeggel, F. C. J. M.; Reinhoudt, D. N. *Chem.−Eur. J.* **2000**, *6*, 1176.

(31) Yasuda, S.; Shigekawa, H.; Suzuki, I.; Nakamura, T.; Matsumoto, M.; Komiyama, M. *Appl. Phys. Lett.* **2000**, *76*, 643

(32) Yu, W. W.; Qu, L.; Guo, W.; Peng, X. *Chem. Mater.* **2003**, *15*, 2854.

(33) Depalo, N.; Comparelli, R.; Curri, M. L.; Striccoli, M.; Agostiano, A. *Synth. Met.* **2005**, *148*, 43;

(34) Depalo, N.; Comparelli, R.; Striccoli, M., Curri, M. L.; Catucci, L.; Agostiano A. *Proc. SPIE Nanotechnology II, Paolo Lugli Ed.* **2005**, *5838*, 245.

(35) Zeng, T.; Claus, R.; Liu, Y.; Zhang, F.; Du, W.; Cooper, K. L. *Smart Mater. Struct.* **2000**, *9*, 801.

(36) Lourenco, J. M. C.; Ribeiro, P. A.; Botelho de Rego, A. M.; Fernandes, F. M. B.; Moutinho, A. M. C.; Raposo, M. *Langmuir* **2004**, *20*, 8103.

(37) http://www.sensir.com/Smiths/InLabSystems/Applications/SD_App19.pdf.

(38) Del Valle, E. M. M. *Process Biochem.* **2004**, *39*, 1033.

(39) Rekharsky, M. V.; Inoue, Y. *Chem. Rev.* **1998**, *98*, 1875.

(40) Spencer, J. N.; He, Q.; Ke, X.; Wu, Z.; Fetter, E. *J. Solution Chem.* **1998**, *27*, 1009.

(41) Shigeyama, M.; Ohgaya, T.; Kawashima, A.; Takeuchi, H.; Hino, T. *Chem. Pharm. Bull.* **2000**, *48*, 617.

(42) Thistlewaite, P. J.; Hook, M. S. *Langmuir* **2000**, *16*, 4993.

(43) Thistlewaite, P. J.; Gee, M. L.; Wilson, D. *Langmuir* **1996**, *12*, 6487.

(44) Gao, M.; Kirstein, S.; Mohwald, H.; Rogach, A. L.; Kornowski, A.; Eychmuller, A.; Weller, H. *J. Phys. Chem. B* **1998**, *102*, 8360.

(45) Sutherland, A. J. *Curr. Opin. Solid State Mater. Sci.* **2002**, *6*, 365 and references therein.

(46) Huh, K. M.; Tomita, H.; Ooya, T.; Lee, W. K.; Sasaki, S.; Yui, N. *Macromolecules* **2002**, *35*, 3775.

(47) Comparelli, R.; Fanizza, E.; Curri, M. L.; Cozzoli, P. D.; Mascolo, G.; Passino, R.; Agostiano, A. *Appl. Catal., B* **2005**, *55*, 81.

(48) Cozzoli, P. D.; Kornowski, A.; Weller, H. *J. Am. Chem. Soc.* **2003**, *125*, 14539.

(49) Rekharsky, M. V.; Schwarz, F. P.; Tewari, Y. B. Goldberg, R. N. *J. Phys. Chem.* **1994**, *98*, 4098.

(50) Ward, M. D. *Chem. Rev.* **2001**, *101*, 1697

α-Cyclodextrin Functionalized CdS Nanocrystals

J. Phys. Chem. B, Vol. 110, No. 35, 2006 **17399**

(51) Sato, K.; Suzuki, I.; Anzai, J. I. *Langmuir* **2003**, *19*, 7406.

(52) Huskens, J.; Mulder, A.; Auletta, T.; Nijhuis, C. A.; Ludden, M. J. W. Reinhoudt, D. N. *J. Am. Chem. Soc.* **2004**, *126*, 6784.

(53) Auletta, T.; Dordi, B.; Mulder, A.; Sartori, A.; Onclin, S.; Bruinink, C. M.; Péter, M.; Nijhuis, C. A.; Beijleveld, H.; Schönherr, H.; Vancso, G. J.; Casnati, A.; Ungaro, R.; Ravoo, B. J.; Huskens, J.; Reinhoudt, D. N. *Angew. Chem., Int. Ed.* **2004**, *43*, 369.

(54) Mulder, A.; Auletta, T.; Sartori, A.; Del Ciotto, S.; Casnati, A.; Ungaro, R.; Huskens, J.; Reinhoudt, D. N. *J. Am. Chem. Soc.* **2004**, *126*, 6627.

(55) Crespo-Biel, O.; Dordi, B.; Reinhoudt, D. N.; Huskens, J. *J. Am. Chem. Soc.* **2005**, *127*, 7594.

(56) de Jong, M. R.; Huskens, J.; Reinhoudt, D. N. *Chem.—Eur. J.* **2001**, *7*, 4164.

(57) Mahalingam, V.; Onclin, S.; Peter, M.; Ravoo, B. J.; Huskens, J.; Reinhoudt, D. N. *Langmuir* **2004**, *20*, 11756.

(58) Tessler, N.; Medevedev, V.; Kazes, M.; Khan; S.; Banin, U. *Science* **2002**, *295*, 1506.

(59) Shipway, A. N.; Katz, E.; Willner, I. *ChemPhysChem* **2000**, *1*, 18.